

Fate, Behavior and Impact Assessment of Biodiesels in Case of an Accidental Spill

Ronan Jezequel, Karine Duboscq, Florence Valladeaud, Stéphane Le Floch
¹CEDRE (Centre de Documentation, de Recherche et d'Expérimentations sur les pollutions accidentelles des eaux), Brest, France
ronan.jezequel@cedre.fr

Abstract

Following an accidental spill of biodiesel in inland waters (France, 2016), Cedre and TOTAL, decided to initiate an experimental study dedicated to understanding the fate and behavior of biodiesel in case of its release in fresh or marine waters. The behaviors of two diesels (B0 and B10) as well as one FAME (fatty acid methyl ester) were studied. The influence of natural weathering processes (evaporation, emulsification, dispersion and photo-oxidation) were assessed at pilot scale in Cedre's flume tank. The different parameters measured on the 15 samples collected during the one-week experiments were: density, viscosity, water content and kinetics of emulsification, emulsion stability, oil adhesion, chemical dispersibility and biodegradability. In addition, the ecotoxicity of the two biodiesels was compared through Microtox® tests (*Vibrio fischeri*).

After one day of weathering, both biodiesels tended to mix with water and form a sort of "emulsion". However, this mixture did not appear stable if the agitation was stopped. After one week of weathering, the total dispersion of B0 and B10 was measured in the water column (formation of a white cloud of droplets). This result suggests that in turbulent condition (i) biodiesels will disperse naturally after a few days of weathering, (ii) mechanical recovery will be effective only during the first 2 to 3 days after the spill occurs. If the agitation was stopped, oil droplets recoalesced to form a slick of weathered biodiesel. Additionally to this recoalescence, a foam-like substance was also observed at the water surface. The formation of this very sticky "foam" (not soluble in solvents such as methylene chloride, hexane, pentane, acetone) was also observed in the field and caused a lot of problems during mechanical recovery. After one week of weathering, natural degradation of B0 and B10 by evaporation and biodegradation processes was close to 60%.

1 Introduction

In France, in 2015, the Energy Transition for Green Growth Act clearly laid out the intent to establish a solid, sustainable energy model on a national and international scale. Faced with depleting fossil fuel reserves, environmental protection requirements and economic challenges, biofuels, manufactured from renewable materials, represent the primary alternative in the transport sector (Ballerini, 2011).

The biodiesels on the European market are first and second generation biofuels, set apart by the feedstock used as the initial biomass. First generation biofuels are mainly manufactured from food resources (i.e. vegetable oils, sugar and starch crops). Oleaginous crops (e.g. rapeseed, soy, sunflower) are the primary source of vegetable oil for producing biodiesel (Knothe and Razon, 2017). Second generation biofuels are manufactured from lignocellulosic biomass, which is plant biomass composed of cellulose, lignin and hemicellulose (e.g. straw and wood). Two families can be identified: (1) "by-product" resources, obtained as a secondary product in the production of a higher value resource (e.g. farming and forestry residues) and (2) "specific" resources, which are specifically cultivated for energy or chemical applications (e.g. triticale, sorghum). Plant and animal oils were targeted as a primary feedstock to offset depleting fossil fuel reserves as they have a similar chemical structure, composed of fatty acids, to that of the diesel fractions of petroleum

(Ballerini, 2011). Nevertheless, the evolution of current engine technologies and the increasingly drastic pollution standards mean that they can no longer be used directly as biodiesel (Hawkins et al., 1983; Murayama et al., 1984; Vellguth, 1983). These fatty acids have had to be transformed to be used in biodiesels. Three main biodiesels have emerged from these transformations: Fatty Acid Methyl Esters (FAME), Hydrotreated Vegetable Oils (HVO) and synthetic biodiesels.

Of these three types of biodiesel, FAMEs have been the focus of the most development efforts, and more specifically methyl esters derived from vegetable oils (Knothe and Razon, 2017; Thomas et al., 2017). It is from these fatty acids that the protocol was originally developed (Chavanne, 1937), resulting in the formation of Vegetable Oil Methyl Esters (VOME). These VOMEs were able to be used as is in old diesel engines (Bruwer et al., 1980; van den Abeele, 1942). Although pure FAMEs can still be used in certain current vehicles fitted with specific equipment, the biodiesels used today are generally composed of a FAME fraction blended with a classic diesel fraction (Prince et al., 2008). These biodiesels are indicated with the letter B followed by the percentage of methyl esters present. In the automotive sector, the proportions generally encountered are 5, 7, 10 and 20 %, respectively B5, B7, B10 and B20 (Prince et al., 2008). Initially set at 7% by the European standard EN 590, the maximum proportion of FAME authorized in a biodiesel today is 10% volume in Europe (AFNOR, 2013). US regulations (ASTM D6751, 2009), on the other hand, accept a FAME percentage of up to 20% volume in biodiesel.

Like all oil products, the weathering of biodiesels released in an aquatic environment is complex as different processes (evaporation, dispersion, emulsification, photo-oxidation, etc.) occur simultaneously. Numerous studies have explored the fate of a spill of such products (Hollebone and Yang, 2009; Hollebone et al., 2008). Recently, Thomas et al. (2017) highlighted the difficulty in predicting the fate and behavior of these biodiesels in the natural environment, as their properties vary not only according to the feedstock used and the presence of additives, but also the proportion of diluted FAME to the classic diesel fraction. In an attempt to overcome this difficulty, and following a spill in France in 2016, Cedre launched an experimental study in 2017 into the behavior of biodiesels in the event of a spill.

2 Materials and Methods

All of the materials and protocols described hereafter are detailed in Guyomarch et al. (2012).

2.1 Flume Test Presentation

Tests at pilot scale were conducted in Cedre's flume tank: the Polludrome (Figure 1). This hydraulic canal, set in an air-conditioned room (0°C to 30°C), consists of a loop through which water can be circulated. The tank is equipped with a wave generator with an adjustable period, a current generator and UV lights. With this equipment, it is possible to weather dedicated oil in similar climatic conditions to those encountered in the oil field from which it is extracted or in the area of shipment. This equipment is used to study the behavior and weathering of chemicals and oils, in particular in the framework of the response to real accidents. Details of the Polludrome are given in Table 1.



Figure 1. Cedre flume tank (Polludrome).

Table 1. Cedre flume tank details

Flume (circulation) length - inner wall	16.4 m
Flume (circulation) length - outer wall	20.2 m
Flume height	1.4 m
Flume width	0.6 m
Wind speed	1.2 m/s
Seawater depth	0.90 m
Surface area	8 m ²
Water volume	7.2 m ³
Temperature	20°C
Oil volume	20 L
Wave height	25 cm
Wave frequency	6 s
Current speed	20 cm/s
Wind speed	3 m/s

The effect of solar rays was simulated by two UV units (Hönle UV technology lamps, 2000 W each). The weathering trials were conducted for a minimum duration of one week and oil samples were regularly taken at the water surface (Table 1). This operation was implemented using a large funnel fitted with a tap to separate the free water from the oil which was then transferred into a separatory funnel. To facilitate sampling, the slick was temporarily concentrated into a thick layer by a boom installed across the width of the tank.

Table 1. Sampling times.

Sample reference	1	2	3	4	5	6	7	8	9	10	11	12	13	14	15	16
Time (h)	1	2	4	6	8	14	24	26	30	48	53	72	77	144	149	168

2.2 Measurement Methods

2.2.1 Flash Point

The flash point was measured according to the NF EN ISO 13736 standard (AFNOR, 2008) by using Anton Paar ABA 4 Flash Point Tester. This parameter was assessed until it reached 100°C, considering this value as a reasonable limit in terms of the risk of ignition of an oil slick.

2.2.2 Density

The density of the samples of surface oil was determined according to the ASTM method ASTM D5002: 2013 (ASTM, 2013) by using an Anton Paar D4500 density meter. This measurement gave the real density of the emulsion that would remain on the sea surface.

2.2.3 Viscosity

The viscosity of the oil samples was measured by establishing the rheological curve using a Haake VT 550 viscosimeter at test temperature, to determine the evolution of the viscosity at dedicated shear rates (e.g. 1, 10, 100 s⁻¹).

2.2.4 Oil Adhesion

The evolution of oil adhesion was measured by weighing the amount of oil that sticks to a given oleophilic plate. This test provides information on the possibility of using oleophilic skimmers.

2.2.5 Emulsification

Emulsification was assessed by measuring the water content in the oil samples in three different ways:

- the water which separated naturally from the oil.
- the water which settled after addition of 0.1% demulsifier (*Demulsip*),
- the water that was distilled using the ISO Dean & Stark method, equivalent to the ASTM D95-05 (2010) Standard Test Method for Water in Petroleum Products and Bituminous Materials by Distillation.

From these measurements, it was possible to determine the kinetics of emulsification as well as the maximum water uptake. The assessment of the stability of the emulsion resulted from the comparison of these data.

2.2.6 Evaporation and Chemical Composition

The saturate and aromatic fractions were analyzed using gas chromatography. Chromatograms of these compounds at different weathering times show the evolution of their distributions. To assess the evaporation rate of the whole oil, a calibration curve was established from samples of the initial oil evaporated in the laboratory by distillation at various temperatures (typically topped at 150, 200 and 250°C).

2.2.7 Oil Biodegradation

A protocol adapted from De Mello et al. (2007) was used to simulate the biodegradation process. Around 10 mg of the fresh crude oil, dissolved in 50 µL of acetone, was biodegraded at the laboratory scale, in a 125 mL glass bottle containing 100 mL of seawater. Nutrients were added to the water, in accordance with the French standard NFT 90-347 (AFNOR, 1990). This method is applied within the French dispersant approval procedure, and aims at assessing the biodegradation of dispersed oil. The hydrocarbon-degrading microorganisms came from a chronically contaminated site. The bottles were loosely plugged with autoclaved cotton wool, placed onto a shaker table, in the dark and

agitated for 28 days. The residual oil was extracted and purified prior to analysis by GC-FID. The GC was an HP 7890N (Hewlett-Packard, Palo Alto, CA, USA equipped with a split/splitless injector (Splitless time: 1 min, flow 50 mL/min) coupled to Flame Ionisation Detector. The injector temperature was maintained at 300°C. The GCFID temperature gradient was from 50°C (1 min) to 300°C (20 min) at 5°C/min. The carrier gas was Hydrogen at a constant flow of 1 ml/min. The capillary column used was an HP-5 MS: 30 m×0.25 mm ID×0.25 µm film thickness.

2.2.8 Quantification of *n*-Alkanes and PAHs in Oil Samples

Each crude oil sample was spiked with internal standards (perdeuterated PAHs) and purified on a cyano micro-column in order to remove polar compounds. Saturated and aromatic compounds were analyzed by Gas Chromatography coupled to Mass Spectrometry (GC-MS). The GC was an HP 7890N (Hewlett-Packard, Palo Alto, CA, USA equipped with a split/splitless injector (Splitless time: 1 min, flow 50 mL/min) coupled to an HP 5975 Mass Selective Detector (MSD) (Electronic Impact: 70 eV, voltage: 1200 V). The injector temperature was maintained at 300°C. The interface temperature was 300°C. The GC/MS temperature gradient was from 50°C (1 min) to 300°C (20 min) at 5°C/min. The carrier gas was Helium at a constant flow of 1 ml/min. The capillary column used was an HP-5 MS: 30 m×0.25 mm ID×0.25 µm film thickness.

PAHs were quantified relatively to the perdeuterated PAHs introduced at the beginning of the sample preparation procedure (perdeuterated eicosane as regards the alkanes). The target molecules, as regards the PAHs, were the 16 PAHs of the US EPA list completed with biphenyl, benzo[e]pyrene and perylene, and also two sulfured aromatics (benzothiophene and dibenzothiophene). For most PAHs, from naphthalene to chrysene, alkylated derivatives characterized by up to 4 additional carbon atoms were also quantified relatively to the parent PAH. Perdeuterated PAHs (Naphthalene-d₈, Biphenyl-d₁₀, Phenanthrene-d₁₀, Chrysene-d₁₂ and Benzo[a]pyrene-d₁₂) and Eicosene C₂₀d₄₂ were obtained from LGC Standards (Molsheim, France). Calibration curves were established from *n*-alkanes and PAH mixtures obtained from Ultra Scientific. These mixtures contained *n*-alkanes from *n*-C₈ to *n*-C₃₂, and as regards PAHs, all the 16 parent PAHs.

3 Results

3.1 Physico-Chemical Properties of the Oils

B0 (diesel) and FAME (Table 2) were provided respectively by Total oil company and VALPRO. B10 was prepared by mixing at ambient temperature these two products at a ratio of 90 / 10 (B0 / FAME).

Table 2. Physico-chemical properties of B0, B10 and FAME.

	Density	Viscosity (mPa.s@20°C / 10 s ⁻¹)	Flash point (°C)	<i>n</i> -alkanes (µg/g)	PAHs (µg/g)
B0	0.838	4	51.0	116 036	7 684
B10	0.842	3	62.5	109 066	7 339
FAME	0.880	5	-	-	-

Figure 2 and Figure 3 present the distribution of *n*-alkanes and PAHs in B0 and B10 biodiesels. These distributions centered around *n*-C₁₃ / *n*-C₁₄ resemble the classic distribution of petroleum diesel products.

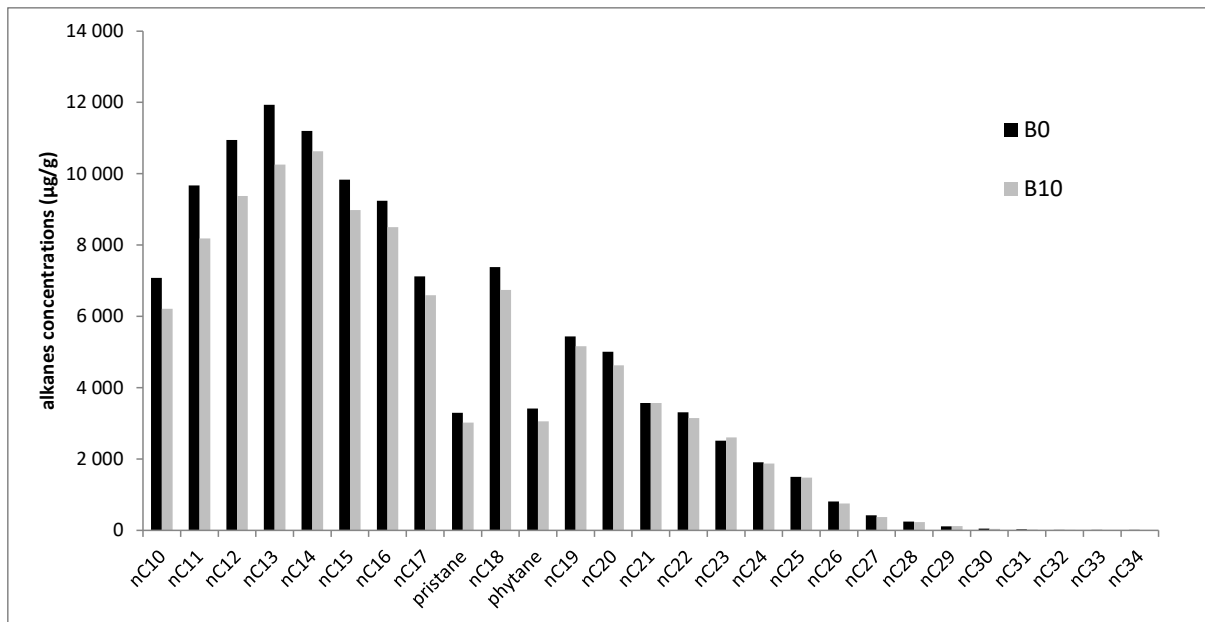


Figure 2. *n*-alkane concentrations in B0 and B10 biodiesels.

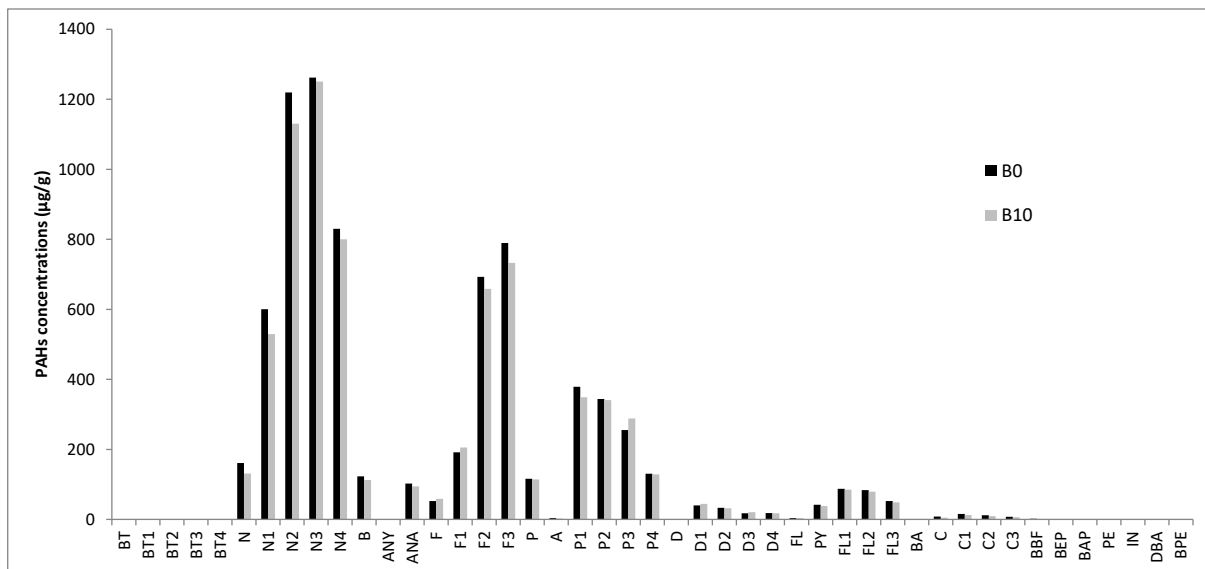


Figure 3. PAH concentrations in B0 and B10 diesels.

3.2 Visual Comparison of B0, B10 and FAME Behaviors

The tables below (Table 3, Table 4) illustrate the changing appearance of the two diesels B0 and B10 during the weathering trial in the flume tank.

Overall, no significant difference was noted between the two products:

- during the first 24 hours, the products did not change visually and remained in the form of slicks covering the whole of the surface of the flume tank.
- between 24 hours and 144 hours (6 days), the biodiesels tended to incorporate water droplets and the product took on an increasingly whitish appearance. This mixture of oil and water was nevertheless very unstable and dependent on continued surface agitation.
- After 6 days of weathering, no slicks were present at the surface, the products were in the form of a plume of droplets distributed evenly throughout the water

column. When agitation was stopped, the surface slick would form again. After settling, the product showed two phases: an upper layer of weathered oil and a sublayer in the form of white agglomerates.

As for the FAME, Table 5 illustrates the changes in the product's appearance during the weathering trial:

- during the first 20 hours, the FAME slick did not evolve;
- between 20 hours and 140 hours, the FAME slick changed color from brown to whitish due to gradual emulsification;
- by the end of the trial, the FAME was partially dispersed in the water. When agitation was stopped, the surface slick would form again.

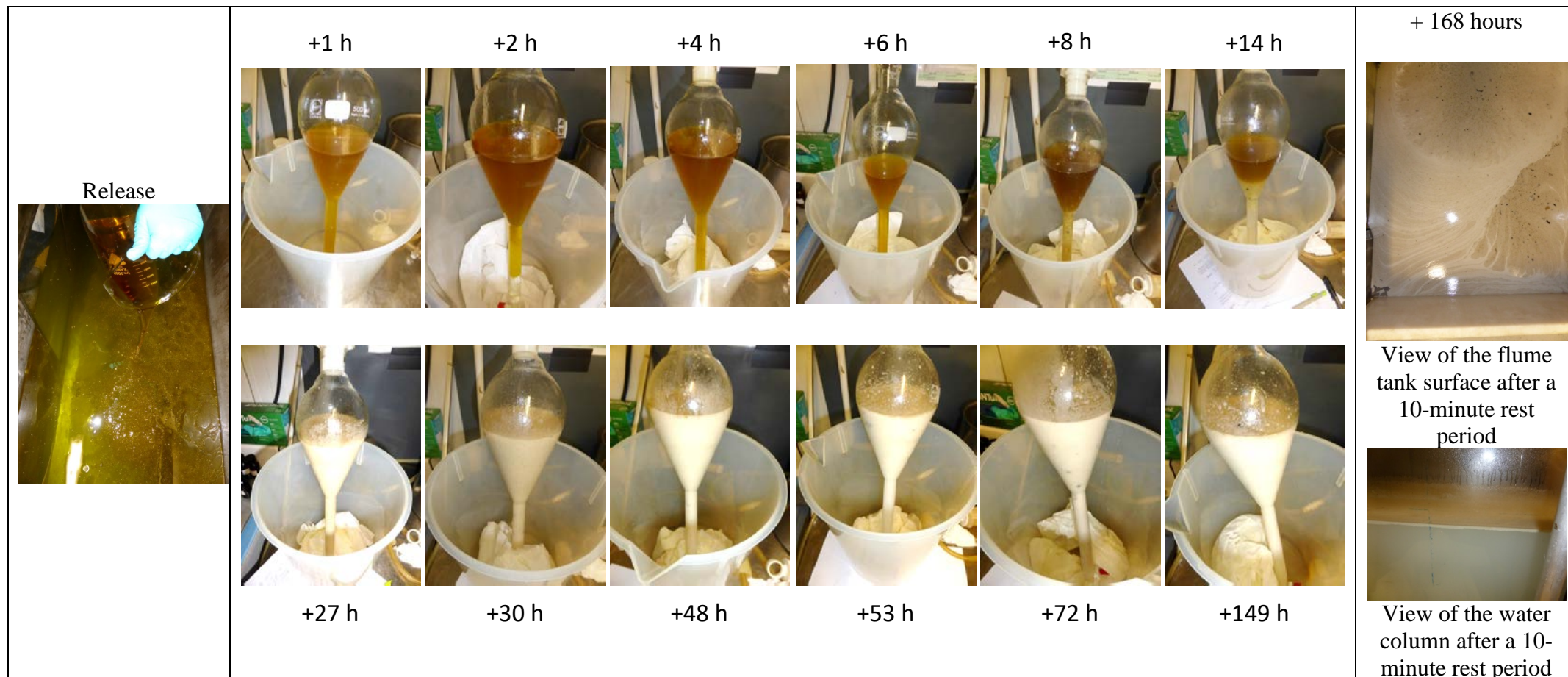
Table 3. Change in appearance of a B0 slick during 1 week of weathering.

<p>Release</p> 	<div style="display: flex; justify-content: space-around; text-align: center;"> +1 h +2 h +4 h +6 h +8 h +24 h </div>  <div style="display: flex; justify-content: space-around; text-align: center;"> +30 h +48 h +53 h +72 h +77 h +149 h </div>	<p>+ 168 hours</p>  <p>View of the flume tank surface after a 60-minute rest period</p>  <p>View of the water column after a 60-minute rest period</p>
	 <p>View of the water column after + 149 hours: immediately after agitation was stopped B0 remained dispersed without the presence of a surface slick. A 60-minute rest period was required to obtain a surface slick.</p>	 <p>View of a sample after a 60-minute settling period</p>

Table 4. Change in appearance of a B10 slick during 1 week of weathering.

<p>Release</p> 	<p>+1 h</p> 	<p>+2 h</p> 	<p>+4 h</p> 	<p>+26 h</p> 	<p>+77 h</p> 
	<p>+ 168 h</p>				
					
	<p>Immediately after agitation was stopped, B10 was in dispersed form</p>	<p>After 20 minutes, a slick started to form</p>	<p>After 60 minutes without agitation, the slick covered the whole of the surface.</p>		<p>View of a sample after being left to settle for 5 minutes (left) and 60 minutes (right)</p>

Table 5. Change in appearance of a slick of FAME during 1 week of weathering.



3.2.1 Evolution of Viscosity

Figure 4 shows the results of the viscosity measurements for B0 and B10. For these two products, an increase in viscosity can be seen. For B0, according to the model applied to the raw results, the maximum viscosity value is estimated at 200 mPa.s.

The FAME did not show such a strong increase in viscosity and it remained below 100 mPa.s. It is worth noting that this evolution follows a sigmoidal pattern, with a sudden increase in viscosity observed between 30 and 48 hours. For B10, due to the variability in results, this evolution in viscosity could not be modelled. Nevertheless, the values obtained tended to remain below 100 mPa.s.

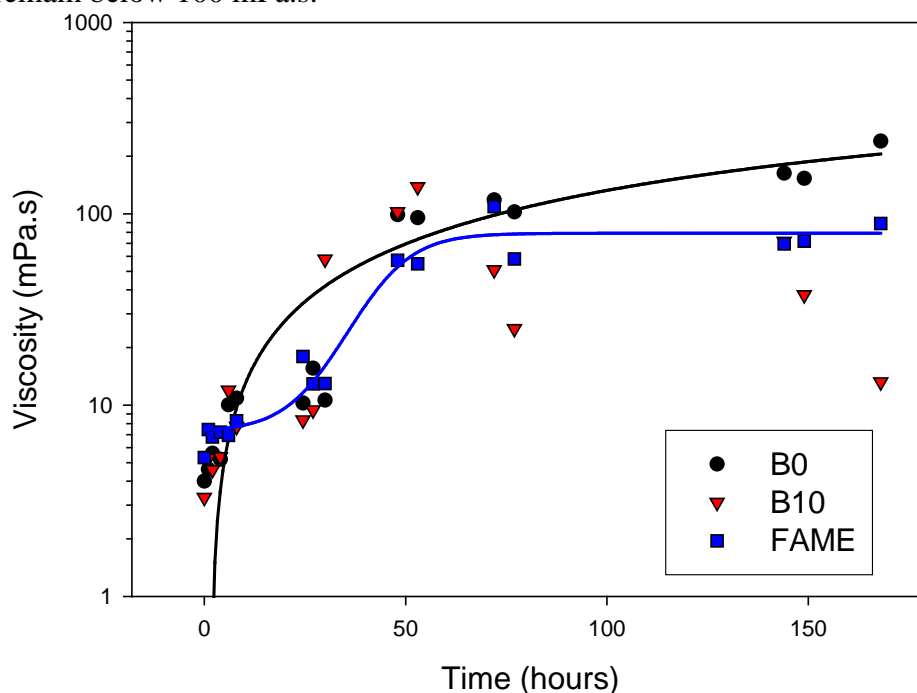


Figure 4. Evolution of viscosity (mPa.s) in B0 and B10 as a function of weathering time (hours).

3.2.2 Evolution of Evaporation

No evaporation of the FAME was detected during these trials.

As for the biodiesels, the evaporation rate was calculated from the changes in the linear alkane distributions. Both products showed exponential growth with maximums of 32% and 40% for B0 and B10 respectively.

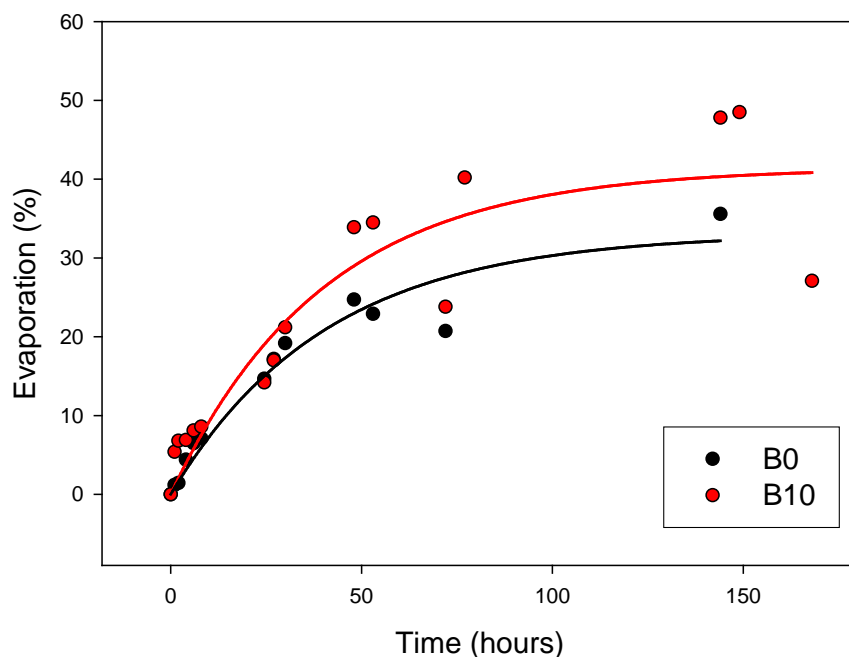


Figure 5. Evolution of evaporation (%) in B0 and B10 as a function of weathering time (hours).

3.2.3 Evolution of Water Content

Figure 6 shows the evolution of water contents for the different products immediately after sampling. As reported for viscosity measurements (Figure 4), the evolution of water content values could only be modelled for B0, which plateaued at a water content of 25%. The variability observed in the results towards the end of the weathering trial suggests the instability of the mixture of B0 / water.

As for B10, the variability in the results (between 80% after 48 hours and 0% after 168 hours) indicates the presence of free water in certain samples due to the instability of the emulsion.

As for the FAME, the emulsions proved to be very unstable. Water was incorporated progressively over the first 3 days of weathering, after which the maximum of 50% was reached.

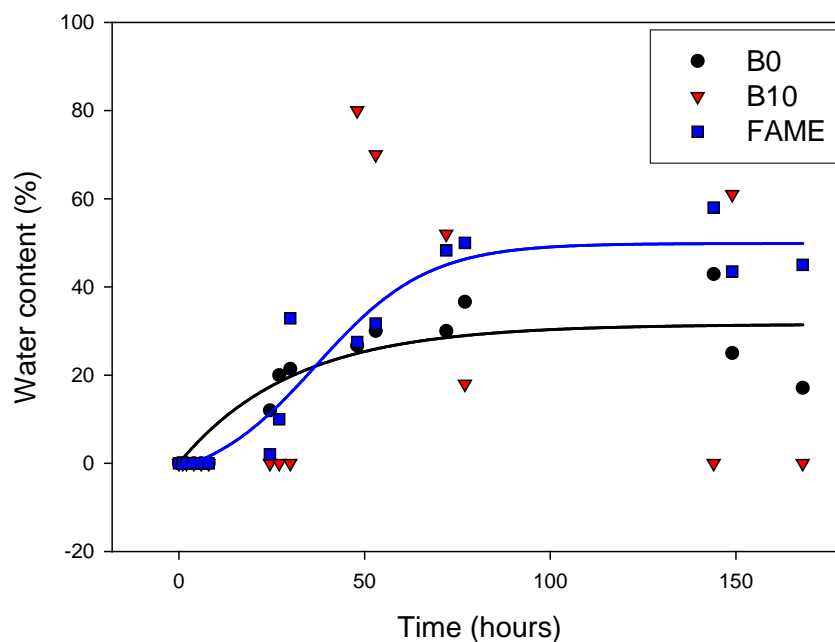


Figure 6. Evolution of water content (%) in B0 and B10 as a function of weathering time (hours).

3.2.4 Evolution of Density

For the diesels, the increasing density (Figure 7) of the water-in-oil emulsions was due to the evaporation of the lightest compounds together with the incorporation of water. For B0, surprisingly, this increase appeared to be almost linear. However, these results should be interpreted with caution due to the difficulty in obtaining an oil sample. As shown by the photographs relating to the changing appearance of the B0 slick (Table 3), even after settling (photo at +168 hours), it was very difficult to obtain a homogeneous sample. For B10, the density values had increased by 3% (0.842 to 0.865) after one week of weathering. For the two products, the density values remained below freshwater densities. Consequently, unless matter in suspension (organic or mineral matter) in the water column is incorporated, a surface slick would not be expected to sink.

For the FAME, the evolution in density follows a sigmoidal pattern in the same way as that of the viscosity values. After 3 days of weathering, the density stabilized at 0.95. Unless matter in suspension is incorporated, this oil is not liable to sink in inland waters.

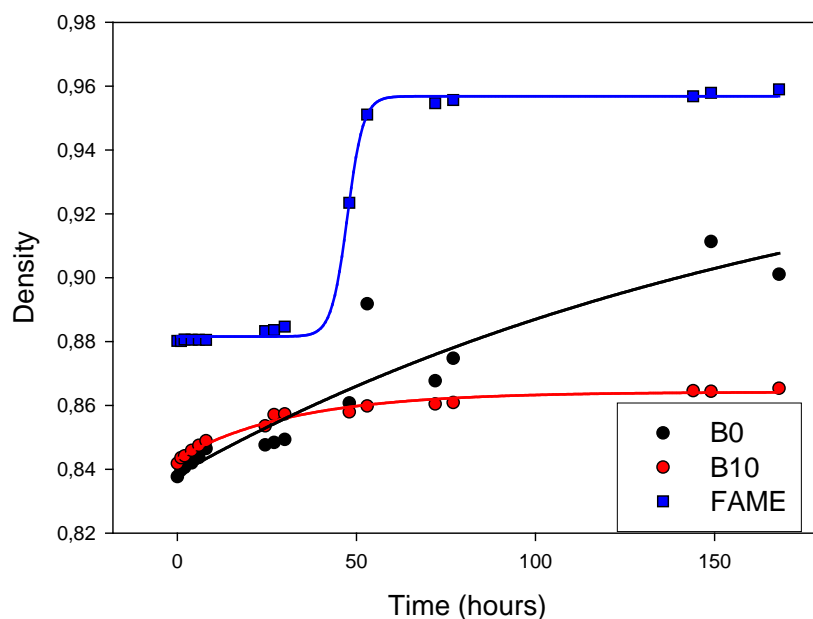


Figure 7. Evolution of density of B0 and B10 as a function of weathering time (hours).

3.2.5 Evolution of Adhesion

Figure 8 shows the results of measurements of adhesion to oleophilic materials. This measurement can be used to quickly determine whether oleophilic skimmers such as drum or disc skimmers would be effective. For instance, for paraffinic oils which tend to solidify at ambient temperatures, this adhesion measurement will be nil, and recovery will involve the use of nets and trawls rather than skimmers. This measurement is also very useful for assessing whether, during weathering, the adhesion capacity may decrease, which would lead to a reduced effectiveness of the skimmers deployed.

As a general rule, adhesion values increase proportionally to viscosity values. In this case, the disparity in the results prevents us from accurately modelling adhesion. Given the small increases in viscosity measured for the two products, it is therefore logical that we find that their adhesion varies very little. Weir skimmers and oleophilic skimmers could therefore be used for both products.

For FAME, there is again little change in adhesion: it goes from 150 g/m² at T0 up to 240 g/m² after 7 days of weathering.

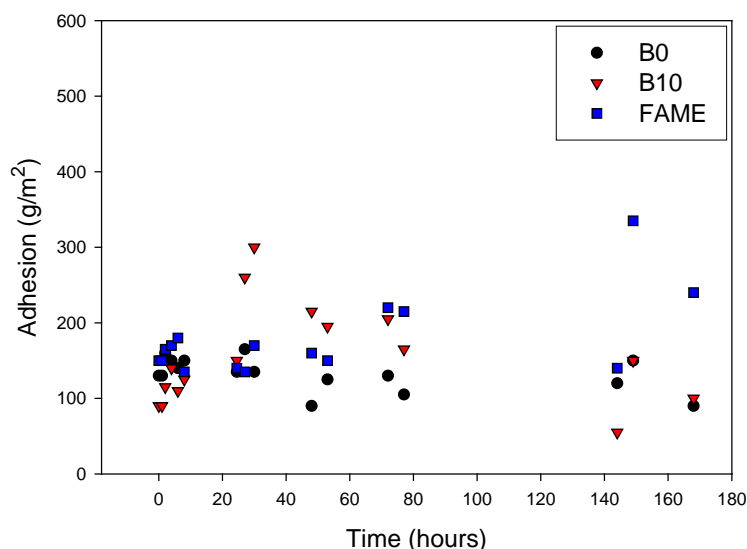


Figure 8. Evolution of adherence (g/m^2) in B0 and B10 as a function of weathering time (hours).

3.2.6 Biodegradability

The fresh oils and their corresponding biodegraded samples were analyzed by GC-FID. This method provides a general view of the oil, from the light compounds (around 10 carbons) to the heaviest (around 30 carbons). In order to establish a reliable mass balance, in addition to the two samples mentioned previously, the residues collected after distillation at 250°C were analyzed (Figure 9, Figure 10, Figure 11).

All the chromatograms were processed in the same way: assuming that the $\text{C}_{26} - \text{C}_{30}$ fraction of the chromatogram remains stable (no biodegradation, evaporation or dissolution), quantities of oil remaining after degradation or evaporation were expressed relatively to this fraction, which allowed the comparison of the different analyses even if injected amounts of oils were different.

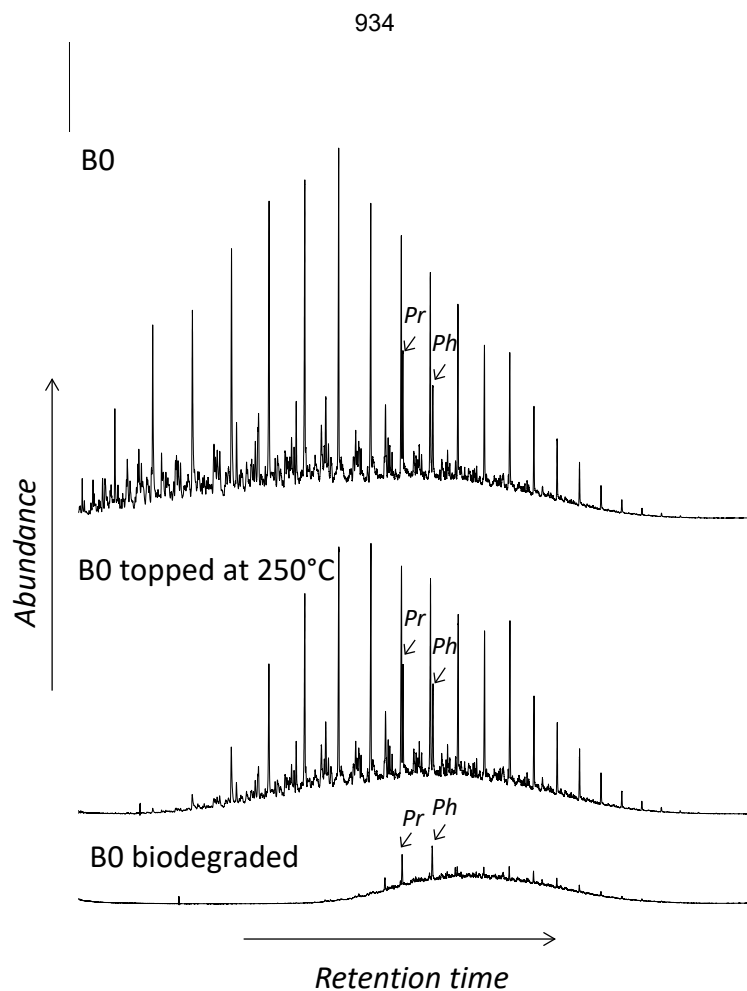


Figure 9. GC/FID chromatograms of the fresh, evaporated and biodegraded B0. *Pr* and *Ph* refer respectively to Pristane and Phytane.

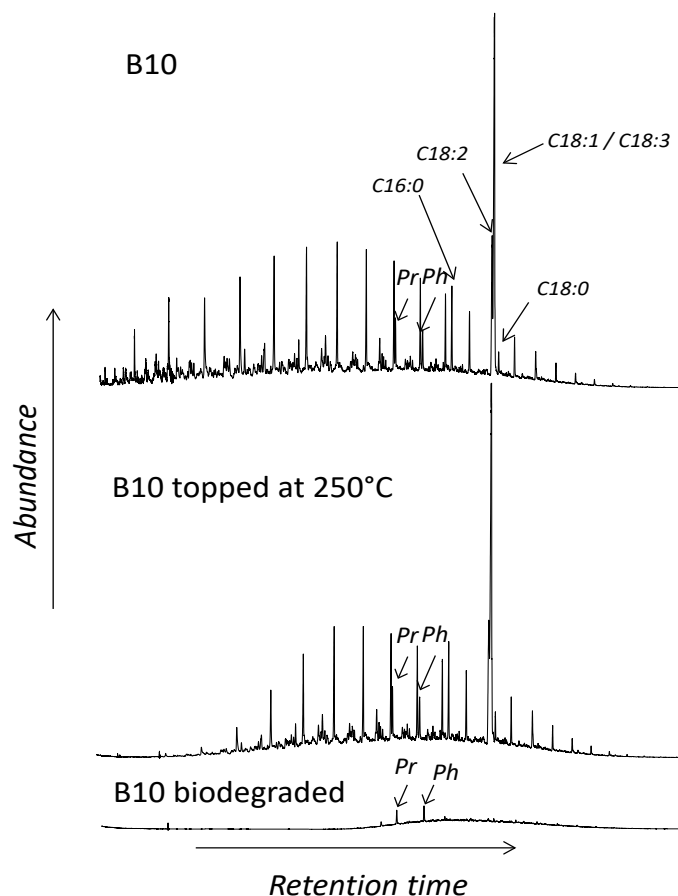


Figure 10. GC/FID chromatograms of the fresh, evaporated and biodegraded B10. *Pr* and *Ph* refer respectively to Pristane and Phytane. C16:0, C18:2, C18:1, C18:3 and C18:0 refer to fatty acid methyl ester compounds.

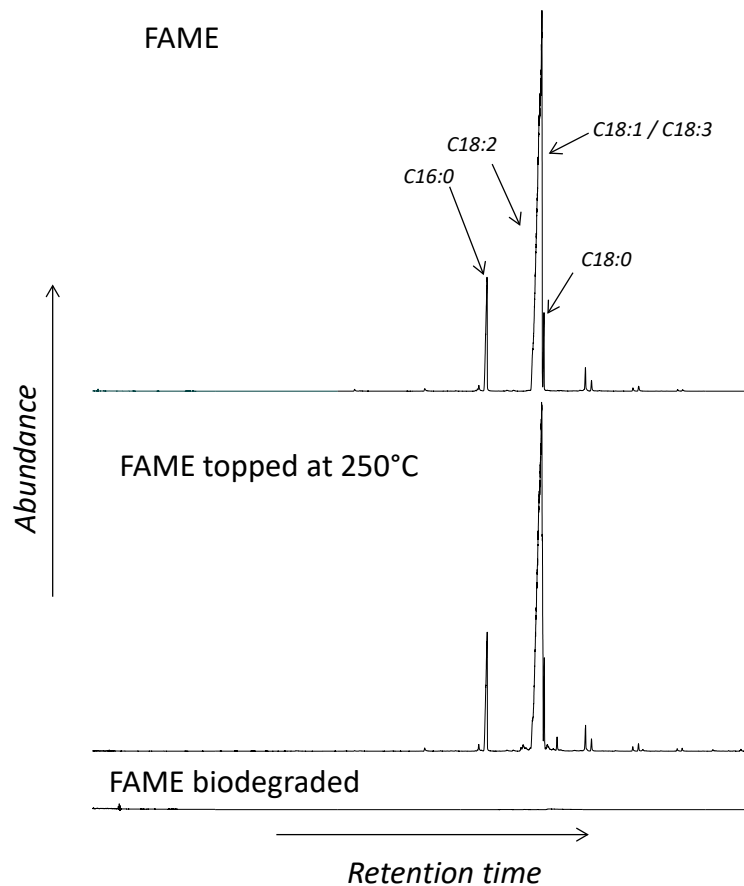


Figure 11. GC/FID chromatograms of the fresh, evaporated and biodegraded FAME. C16:0, C18:2, C18:1, C18:3 and C18:0 refer to fatty acid methyl ester compounds.

The biodegradation rates were calculated assuming that the evaporation process would be completed, and were therefore calculated relatively to the 250°C+ residues. The results are presented in Figure 12. After 28 days of experimentation, biodegradation of FAME oil appeared almost completed. This is consistent with previous studies (Hollebone et al., 2009).

For biodiesels, the addition of FAME in B0 increases its biodegradability: 29% for B0 compared to 39% for B10. This concurs with the results obtained by Prince et al. (2008).

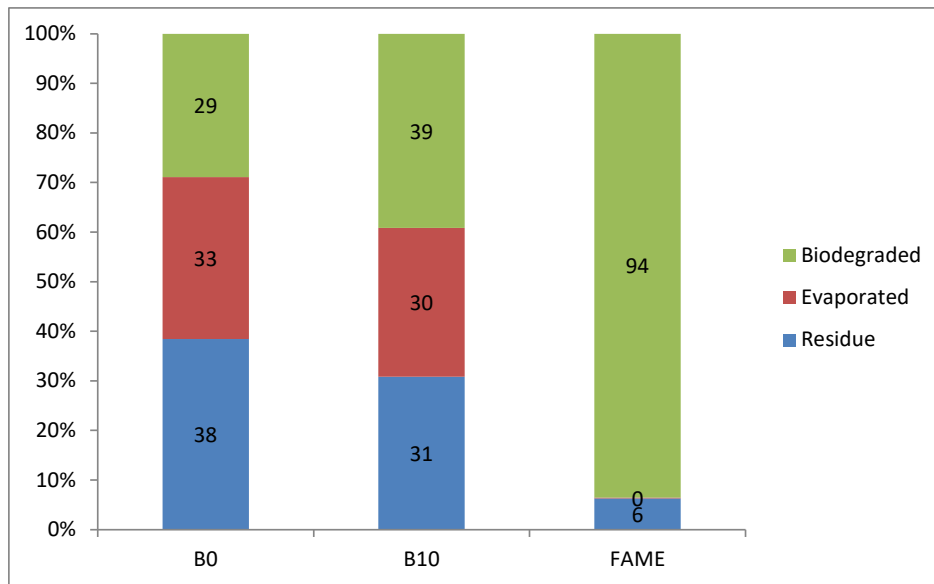


Figure 12. Mass balance of the B0, B10 and FAME samples.

4 Conclusion and Future Prospects

Several conclusions can be drawn from this experimental weathering study (7 days) conducted on two oils (B0 and B10) and one FAME:

- persistence in the environment: around 30% of a biodiesel blend will evaporate. In terms of biodegradation, at least 30% will biodegrade and this share increases with the proportion of FAME used to produce the biodiesel. FAME does not evaporate but it is very sensitive to biodegradation.
- density: for the 3 products, the density values remained below the densities of freshwater and seawater. Consequently, unless matter in suspension (organic or mineral matter) in the water column is incorporated, a surface slick would not be expected to sink.
- viscosity: the values remained below 200 mPa.s for B0, 100 mPa.s for B10 and reached 400 mPa.s for FAME. Given these values, weir skimmers or oleophilic skimmers can be used to recover even very weathered slicks.
- Mixture of oil and water: all 3 products tend to incorporate water droplets quickly, with FAME reaching a maximum of 50%. These mixture nevertheless remain very unstable and a settling period of a one hour is sufficient to separate the aqueous and organic phases so as to significantly decrease the volumes to be treated.
- agglomeration: the appearance of white agglomerates was observed during the trials in the flume tank for both biodiesels. Given the issues encountered during a real spill (Poncet et al., 2019), characterization work should be implemented to explain this phenomenon.
- Transfer into the water column: this was observed after 6 days of weathering in the form of a white cloud of droplets. In real-life conditions, this phenomenon would occur in watercourses characterized by an uneven riverbed and/or a strong flow. In such cases, the sediment is at risk of contamination and recovery of the diesel would be almost impracticable unless a settling basin is available to contain the slick.
- adhesion varies very little for both products. Weir skimmers and oleophilic skimmers could therefore be used for both products.

This experimental study is to be further pursued by studying new generation biodiesel B30 produced from the basic diesel B0 blended with 30% HVO (Hydrogenated Vegetable Oil).

5 Acknowledgements

This study was supported by the MTES (Ministère de la Transition Ecologique et Solidaire) and TOTAL oil company.

6 References

AFNOR NF EN ISO 13736 (Juillet 2013), “Détermination du point d'éclair - Méthode Abel en vase clos”, 2013.

AFNOR NF EN 14214, « Produits pétroliers liquides - Esters méthyliques d'acides gras (EMAG) pour moteurs diesel et comme combustible de chauffage - Exigences et méthodes d'essai - Carburants pour automobiles », 2013.

AFNOR NFT 90-347, Essais des eaux - Produits dispersants - Évaluation en milieu aqueux de l'action inhibitrice sur la biodégradabilité du pétrole, 1990.

ASTM, “Standard Specification for Biodiesel Fuel Blend Stock (B100) for Middle Distillate Fuels”, ASTM D6751-09, American Society for Testing and Materials International, West Conshohocken, PA, 2009.

ASTM, “Standard Test Method for Density and Relative Density of Crude Oils by Digital Density Analyzer”, ASTM D5002 - 13. American Society for Testing and Materials International, West Conshohocken, PA, 2013.

ASTM, “Standard Test Method for Water in Petroleum Products and Bituminous Materials by Distillation”, ASTM D95-05 (2010), American Society for Testing and Materials International, West Conshohocken, PA, 2010.

Ballerini, D., *Les biocarburants: répondre aux défis énergétiques et environnementaux des transports*, TECHNIP. ed, IFP Energies nouvelles – Publications, 416 p., 2011.

Bruwer, J.J., F.J.C. Hugo, and F.J.C., Hawkins, “Sunflower seed oil as an extender for diesel fuel in agricultural tractors”, *Presented at the Symposium of the South African Institute of Agricultural Engineers*, Aberdeen, 7 p., 1980.

Chavanne, G., “Procédé de transformation d'huiles végétales en vue de leur utilisation comme carburants”, Belgian patent 422,877, 1937.

De Mello, J.A., C.A. Carmichael, E.E. Peacock, R.K. Nelson, J. Samuel Arey, and C.M. Reddy, “Biodegradation and environmental behavior of biodiesel mixtures in the sea: An initial study”, *Marine Pollution Bulletin*, 54: 894–904, 2007.

Guyomarch J., S. Le Floch and R. Jezequel, “Oil Weathering, Impact Assessment and Response Options Studies at the Pilot Scale: Improved Methodology and Design of a New Dedicated Flume Test”, in *Proceedings of the thirty-fifth AMOP Technical Seminar on Environmental Contamination and Response*, Environment Canada, Ottawa, ON, 2012.

Hawkins, C., J. Fuls, and F. Hugo, “Engine Durability Tests with Sunflower Oil in an Indirect Injection Diesel Engine”, in *Technical Papers. Presented at the 1983 SAE International Off-Highway and Powerplant Congress and Exposition*, SAE Technical Papers. <https://doi.org/doi.org/10.4271/831357>, 1983.

Jézéquel, R., K. Duboscq, F. Valladaud, and S. LeFloch, Fate, Behaviour, and Impact Assessment of Biodiesels in Case of an Accidental Spill, Proceedings of the Forty-second AMOP Technical Seminar, Environment and Climate Change Canada, Ottawa, ON, Canada, pp. 919-939, 2019.

Hollebone, B. and Z. Yang, “Biofuels in the environment: A review of behaviours, fates, effects and possible remediation techniques”.in Proceedings of the 32nd AMOP Technical Seminar on Environmental Contamination and Response 1, 127–139. 2009.

Hollebone, B.P., B. Fieldhouse, M. Landriault, K. Doe, and P. Jackman, “Aqueous solubility, dispersibility and toxicity of biodiesels”, in *Proceedings of the 2008 International Oil Spill Conference Proceedings*, pp. 929–936. <https://doi.org/10.7901/2169-3358-2008-1-929>. 2008.

Knothe, G. and L.F. Razon, “Biodiesel fuels. Progress in Energy and Combustion”, *Science*, 58:36–59. <https://doi.org/10.1016/j.pecs.2016.08.001>, 2017.

Murayama, T., Y.T. Oh, N. Miyamoto, T. Chikahisa, N. Takagi, and K. Itow, “Low carbon flower buildup, low smoke, and efficient diesel operation with vegetable oils by conversion to mono-esters and blending with diesel oil or alcohols”, in: *SAE Technical Papers. Presented at the International Off-Highway and Powerplant Congress and Exposition*. <https://doi.org/10.4271/841161>. 1984.

Poncet, F., R. Jezequel, I. Calvez, M. Laurent, W. Giraud, and J. Receveur, “Recent pollution case study: Biodiesel Spill of inland waters related to a pipeline accidental rupture: response and impact evaluation”, in *Proceedings of the 42nd AMOP Technical Seminar on Environmental Contamination and Response*, Environment and Climate Change Canada, Ottawa, ON, 2019.

Prince, R.C., C. Haitmanek, and C.C. Lee, “The primary aerobic biodegradation of biodiesel B20”, *Chemosphere*, 71:1446–1451. <https://doi.org/10.1016/j.chemosphere.2007.12.010>. 2008.

Thomas, A.O., M.C. Leahy, J.W.N. Smith, and M.J. Spence, “Natural attenuation of fatty acid methyl esters (FAME) in soil and groundwater”, *Quarterly Journal of Engineering Geology and Hydrogeology*, 50:301–317. <https://doi.org/10.1144/qjegh2016-130>. 2017.

van den Abeele, M., “L’huile de palme: matière première pour la préparation d’un carburant lourd utilisable dans les moteurs à combustion interne”, *Chemical Abstract* 33. p1., 1942.

Vellguth, G., “Performance of Vegetable Oils and their Monoesters as Fuels for Diesel Engines”, *Presented at the 1983 SAE International Off-Highway and Powerplant Congress and Exposition*, SAE Technical Papers, p. 12. <https://doi.org/doi.org/10.4271/831358>. 1983.